FOSSEE, IIT Bombay
OpenFOAM Case Study Project
January 23, 2026

Non Newtonian Flow Past 2D Cylinder

Subbulakshmi[1] Pranay Pandey[2] Tushar Chourushi[3] Chandan Bose[4],
[1]Aerospace Engineering, Amrita Vishwa Vidyapeetham, Tamil Nadu, India
[2]FOSSEE, Indian Institute of Technology, Bombay, India
[3]Associate Professor, Department of Aerospace Engineering,
MIT Art, Design and Technology University, Pune, Maharashtra, India
[4]Assistant Professor, Aerospace Engineering,
College of Engineering and Physical Sciences, University of Birmingham, UK

Abstract

This study presents a numerical investigation of two-dimensional (2D) laminar flow of non-Newtonian fluids past circular cylinder using the open-source CFD software `OpenFOAM`. Simulations are performed using `nonNewtonianIcoFoam` solver to study and compare the behaviour of two commonly used non-Newtonian fluid models, namely the Power Law and Carreau models. Flow parameters such as lift coefficient (C_l), drag coefficient (C_d) and Strouhal number (St) are evaluated from the simulations and validated against benchmark results available in the literature. The comparison provides an assessment of the accuracy of the numerical setup and evaluates the suitability of these rheological models for simulating non-Newtonian flow past bluff bodies.
Keywords: Non-Newtonian fluids, Power-law model, Carreau model

1 Introduction

The investigation of non-Newtonian fluid dynamics is essential for analyzing complex materials that exhibit a non-linear relationship between shear stress and the rate of deformation. Unlike Newtonian fluids, non-Newtonian fluids have a variable apparent viscosity that depends on local flow conditions. These fluids are typically categorized by their behavior as either shear-thinning or shear-thickening. According to Chhabra and Richardson [1], the rheological properties of these fluids require specialized constitutive models to accurately predict momentum transport and energy dissipation in both industrial and biological applications.

The interaction of these fluids with a 2D cylinder serves as a key benchmark for analyzing flow properties. The presence of variable viscosity fundamentally changes the flow behavior, particularly by shifting the critical Reynolds number (Re_c). It is the number at which the transition from steady to unsteady periodic vortex shedding occurs. For example, shear-thinning effects tend to destabilize the wake and lower the threshold for vortex shedding, while shear-thickening behavior can significantly delay separation and increase Re_c [2]. Understanding these dynamics is crucial for optimizing the structural integrity and thermal efficiency of components operating in non-Newtonian environments.

2 Problem Statement

The flow of varying Reynolds numbers (Re) is simulated around a 2D stationary cylinder. The fluid is modeled using the Power Law and Carreau models. An unconfined domain surrounding a cylinder with a diameter of 1 meter in the x-y plane is used for simulations. The geometry is illustrated in Figure 1.

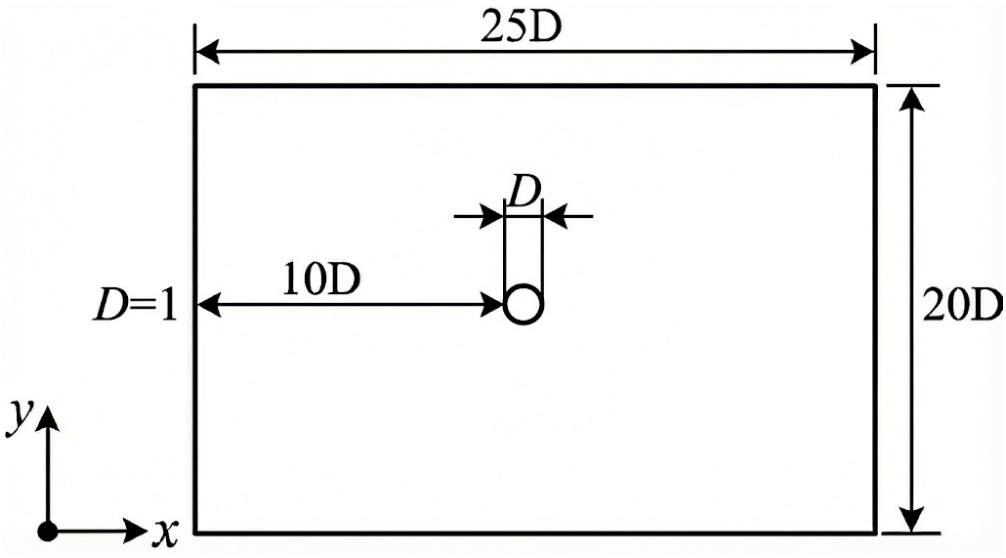

Figure 1: Geometry Description

3 Governing Equations and Rheological Models

The governing equations for 2D incompressible, laminar and non-Newtonian flow are given as follows:

3.1 Governing Equations

Continuity Equation
In the case of incompressible flow, conservation of mass is given by:

$$\nabla \cdot \mathbf{U} = 0 \tag{1}$$

where the velocity vector is defined as

$$\mathbf{U} = (u,\, v)$$

representing the velocity components in the x and y directions, respectively.
Momentum Equation
The conservation of momentum for an incompressible flow is expressed as:

$$\rho \left(\frac{\partial \mathbf{u}}{\partial t} + \mathbf{u} \cdot \nabla \mathbf{u} \right) = -\nabla p + \nabla \cdot \tau \tag{2}$$

where ρ is the fluid density, p is the pressure, and τ is the stress tensor. The stress tensor is related to the velocity gradients through the apparent viscosity as:

$$\tau = 2\,\eta(\dot{\gamma})\,\mathbf{D} \tag{3}$$

where $\eta(\dot{\gamma})$ is the viscosity depending on the shear rate. The rate-of-strain tensor **D** is defined as:

$$\mathbf{D} = \frac{1}{2}\left(\nabla\mathbf{u} + (\nabla\mathbf{u})^T\right) \tag{4}$$

3.2 Viscosity Models

The Power Law and Carreau Models are discussed below.

3.2.1 Power Law (Ostwald–de Waele) Model

The Power Law model, is a commonly used constitutive relation for describing non-Newtonian fluid behavior. The apparent viscosity is expressed as a function of the shear rate as

$$\eta = K\,\dot{\gamma}^{\,n-1} \tag{5}$$

where

- K is the **consistency index** (Pa · s^n)
- n is the **flow behavior index**

Based on the value of n, fluids are classified as

- **Shear-thinning** fluids for $n < 1$,
- **Newtonian** fluids for $n = 1$,
- **Shear-thickening** fluids for $n > 1$.

The generalized Reynolds number for flows governed by this model is defined as

$$Re = \frac{\rho\,U^{2-n}\,D^{n}}{K} \tag{6}$$

where U is the characteristic velocity, and D is the characteristic length scale. The Power Law model is computationally simple and effective over a limited range of shear rates. At very low or very high shear rates the behavior of the fluid is not captured accurately.

3.2.2 Carreau Model

Using the Carreau model, the viscosity response of the fluid changes gradually, remaining nearly constant at low shear rates and decreasing with increasing shear rate due to shear-thinning effects. The apparent viscosity is given by:

$$\eta = \eta_\infty + (\eta_0 - \eta_\infty)\left[1 + (\lambda\dot{\gamma})^2\right]^{\frac{n-1}{2}} \tag{7}$$

where

- η_0 is the **zero-shear viscosity** (Pa · s),
- η_∞ is the **infinite-shear viscosity** (Pa · s),
- λ is the **relaxation time** (s),
- n is the **power-law index**.

Carreau Number
The Carreau number (Cu) represents the ratio of fluid relaxation time and the characteristic flow time scale and is defined as:

$$Cu = \frac{\lambda U}{D} \tag{8}$$

where U represents the characteristic velocity and D denotes the characteristic length scale. For $Cu \ll 1$, the fluid response is close to Newtonian and the viscosity approaches the zero-shear value η_0, while for $Cu \gg 1$, shear-thinning effects dominate.

Reynolds Number
The Reynolds number for the non-Newtonian flow is defined using the zero-shear viscosity as:

$$Re = \frac{\rho U D}{\eta_0} \tag{9}$$

where η_0 is the zero-shear viscosity.

4 Simulation Procedure

The case file contains three directories: 0, constant, and system. In the 0 folder the boundary and initial conditions for the flow variables, such as velocity and pressure, corresponding to a laminar flow case are present.

The constant folder stores the mesh and physical properties. The mesh files are located in the polyMesh folder, where the boundary file is modified to assign the appropriate patch types. Although Gmsh allows grouping and naming of boundaries, the exported mesh assigns them as generic patches, which must be corrected after mesh import. The viscosity parameters are specified in the transportProperties file.

The system directory contains the solver control and numerical settings. The decomposeParDict file is included to enable parallel computation.

To execute the case, Allclean and Allrun scripts are provided. Allclean cleans the case directory by removing temporary files and previous simulation data. And, Allrun contains all the necessary commands to fully automate and run the simulation. The overall directory structure is presented in Table 1.

Table 1: OpenFOAM Case File Directory Structure

Directory	**Contents**
0	p, U
constant	polyMesh transportProperties
system	controlDict decomposeParDict fvSchemes fvSolution

4.1 Geometry and Mesh

The geometry features a cylinder with a diameter of 1 meter, accompanied by a refinement region measuring $2\sqrt{2}$ meters. The mesh for this geometry was created using Gmsh software. The blocks and mesh are illustrated in Figure 2. Following the mesh creation, it was exported to the case file, and the patch type was renamed accordingly.

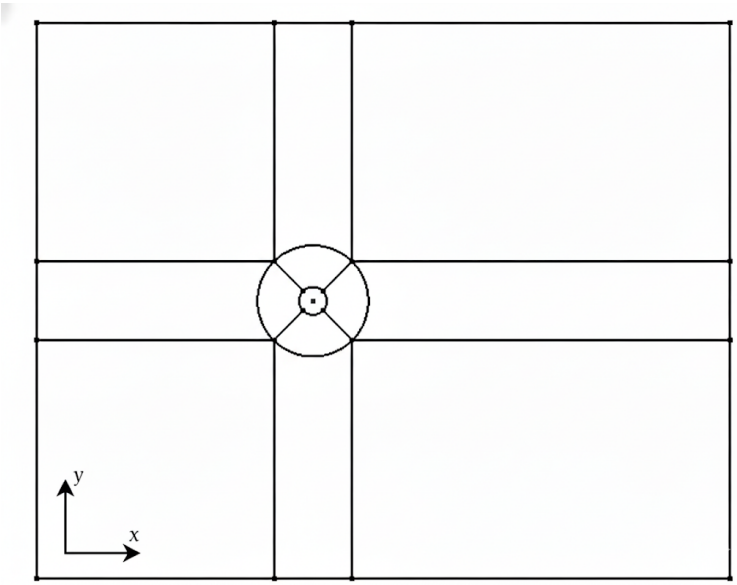

Figure 2: Block Description

4.2 Initial and Boundary Conditions

The specified initial and boundary conditions for the simulation are given below. The inlet velocity (u) for different cases was calculated using the Reynolds number formula of the model.

Table 2: Boundary Conditions Used in the Simulation

Patch Name	**Pressure (p)**	**Velocity (U)**
Inlet	zeroGradient	$(u, 0, 0)$
Outlet	fixedValue (0)	zeroGradient
Cylinderwall	zeroGradient	noSlip
Upperwall	symmetryPlane	symmetryPlane
Lowerwall	symmetryPlane	symmetryPlane
Front and back	empty	empty

4.3 Solver

The `nonNewtonianIcoFoam` solver is designed for laminar, unsteady flows of non-Newtonian fluids, where viscosity varies with shear rate. It solves the Navier–Stokes equations for velocity and ensures continuity by iteratively correcting the pressure field. Viscosity is updated at each time step using models such as the Power Law. The outcome of the simulations are highly sensitive to the chosen viscosity parameters. Accurate model parameters are crucial for simulating shear-dependent internal and external flows effectively.

5 Results and Discussions

5.1 Grid Independence Study

A grid independence analysis was performed for the Power Law model at a Reynolds number of 100, with a flow behavior index of $n = 1.8$. The mean drag coefficient (C_d) was used as the comparison parameter to evaluate grid convergence. Four mesh resolutions were considered in the analysis. The mesh containing 312,500 cells was ultimately selected for further study because the difference in the drag coefficient was on the order of 10^{-3} and remained consistent with further refinements.

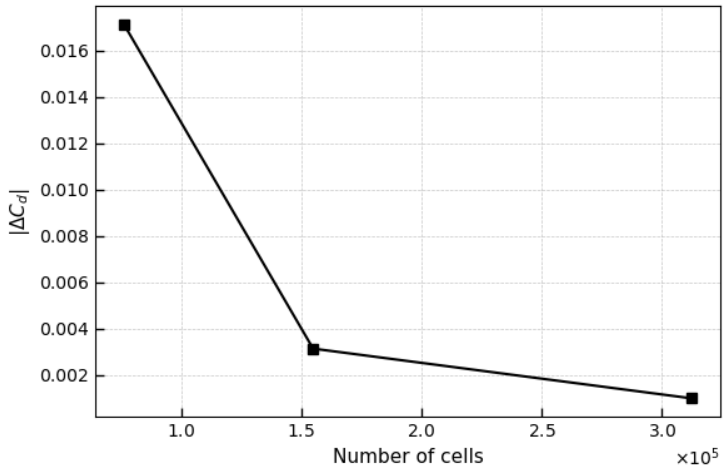

Figure 3: Grid Independence

Table 3: Grid Independence Study for Drag Coefficient

Number of Cells	C_d
76,200	1.7103
154,880	1.69004
312,500	1.69219
648,000	1.69317

5.2 Time Independence study

A time independence analysis was performed for the Carreau viscosity model at a Reynolds number of $Re = 10$ and a flow behavior index of $n = 0.4$. The Carreau model was selected due to its increased sensitivity to variations in time steps compared to other viscosity models. Three different time-step scenarios were simulated. A time step of $\Delta t = 0.0005$ was chosen for the further study, as the difference between consecutive values of C_d was on the order of 10^{-3}, indicating that the results were independent of the time step.

Table 4: Time Step Independence Study

Time Step	C_d
0.0025	1.66458
0.0005	1.66646
0.0001	1.666416

5.3 Power Law Model

The Power Law model was assessed using two different Reynolds number conditions to account both shear-thinning and shear-thickening behavior. The obtained results were evaluated against the

benchmark data reported in [2]. A comparison table presents the mean drag coefficient (C_d) from the simulations, the benchmark values, and the corresponding percentage error. In all instances, the error remained below 5

As discussed in [2], the flow behavior index n is varied while maintaining a constant Reynolds number. The drag coefficient was observed to increase as n increased. A similar trend is observed when the Reynolds number is varied while keeping n fixed. Furthermore, the solver demonstrates sensitivity to the model parameters, as the error percentage remains relatively consistent for shear-thinning cases, while a higher error is noted for shear-thickening cases.

Table 5: Comparison of Drag Coefficient with Benchmark Data

Re	n	C_d **(Benchmark)**	C_d **(Simulation)**	**Error(%)**
40	0.6	1.3576	1.35057	< 1
40	1.8	1.8095	1.86626	3.18
100	0.4	1.1345	1.129621	< 1
100	1.8	1.6294	1.69219	3.8

5.4 Carreau Model

The Carreau model was assessed by simulating the flow at a Reynolds number of 10 under shear-thinning conditions, as literature data for this model is limited. The results include obtained drag coefficient, benchmark values, and the corresponding error percentages. The error remained below 5%, demonstrating good agreement with reference data. Consistent with the behavior discussed for the Power Law model in [3], increasing the flow behavior index n results in a higher drag coefficient. The same trend is observed in the present analysis.

Table 6: Comparison of Benchmark and Obtained Drag Coefficient at $Re = 10$

n	C_d **(Benchmark)**	C_d **(Simulation)**	**Error (%)**
0.4	1.22	1.188	3.2
0.6	1.67	1.6385	1.8
0.8	2.20	2.23	1.36

6 Conclusion

In this study, the `nonNewtonianIcoFoam` solver was used to simulate 2D laminar flows of non-Newtonian fluids around a circular cylinder. The primary goal was to verify and validate the accuracy of the solver. Verification involved conducting a grid independence study with four different mesh resolutions, and the mesh with 312,500 cells was selected. A time-step independence study was also carried out, as the Carreau model showed sensitivity to the time step size. A time step of 0.0005 was chosen for optimal results.

The simulations were performed using both the Power Law and Carreau models across different Reynolds numbers and flow behavior index (n) values. The results were then compared with benchmark data from existing literature, revealing that the error percentage remained below 5% in

both cases. The variation of drag coefficient in relation to the Reynolds number and n aligned with trends observed for flow around a cylinder. Furthermore, the dependence of the solver to model parameters was evident, as the error increased for the shear-thickening case with $n = 1.8$ in the Power Law model.

Overall, the results show that the simulation framework employed in this study is capable of accurately capturing the characteristics of non-Newtonian fluids, making it suitable for further investigations in this area.

References

[1] RP Chhabra and JF Richardson. Non-newtonian fluid behaviour. *Non-newtonian flow and applied rheology*, pages 1–55, 2008.

[2] V. K. Patnana, R. P. Bharti, and R. P. Chhabra. Two-dimensional unsteady flow of power-law fluids over a cylinder. *Chemical Engineering Science*, 64(12):2978–2999, 2009.

[3] A. Pantokratoras. Steady flow of a non-newtonian carreau fluid across an unconfined circular cylinder. *Meccanica*, 51(4):1007–1016, 2016.